THE PENNSYLVANIA STATE UNIVERSITY
SCHREYER HONORS COLLEGE

DEPARTMENT OF ENGINEERING SCIENCE AND MECHANICS

DESIGN OF A TRI-PHASIC BIOMECHANICAL MODEL DESCRIBING HEALTHY AND CANCEROUS TISSUE

KATHRYN I. BARBER

Spring 2011

A thesis
submitted in partial fulfillment
of the requirements
for a baccalaureate degree
in Engineering Science
with honors in Engineering Science

Reviewed and approved* by the following:

Dr. Corina Drapaca
Assistant Professor of Engineering Science and Mechanics
Thesis Supervisor

Dr. Judith Todd
P.B. Breneman Department Head Chair
Professor, Department of Engineering Science and Mechanics
Honors Advisor

Dr. Patrick Drew
Assistant Professor of Engineering Science and Mechanics
Faculty Reader

* Signatures are on file in the Schreyer Honors College and Engineering Science and Mechanics Office.

Abstract

The ever-growing field of non-invasive diagnostic technologies is continually providing new insights into *in vivo* biological processes, requiring joint efforts among researchers in medicine, science, and engineering. One of these emerging technologies, Magnetic Resonance Elastography (MRE), uses an imaging technique to measure the elasticity of biological tissues subject to mechanical stresses. The resulting strains are measured using Magnetic Resonance Imaging (MRI) and the related elastic modulus is computed from models of tissues mechanics. The elastic modulus contains important information about the pathology of the imaged tissues. For example, fibrotic tissue in the liver is much less elastic than healthy tissue, and malignant tumors are more elastic than benign tumors. Thus, MRE can help in tumor detection, determination of characteristics of disease, and in assessment of rehabilitation. The biomechanical models used so far in MRE are classic macroscopic models which do not incorporate any relevant information about the electro-chemical processes that take place in the microstructure of the tissue. A novel multiscale model is presented that may differentiate not only between healthy and diseased tissues but also between benign and malignant tumors. The tissue is modeled as a triphasic material of porous, viscoelastic solid filled with interstitial fluid and dissolved ions. A recently-developed homogenization technique for materials with evolving microstructure was used to approximate a periodic microscopic structure.

Keywords: computational modeling, tri-phasic model, cancer, brain tissue, magnetic resonance elastography, non-invasive diagnostic procedures

Table of Contents

List of Figures

List of Variable Notations

Superscripts or subscripts of s, w, +, or – indicate solid phase, liquid (water) phase, and cations or anions in the ion phase. Subscript zero indicates a reference or characteristic quantity. A tilde over the variable indicates that it is a dimensionless quantity.

Quantity	Notation
total stress of the mixture (tissue)	$\boldsymbol{\sigma}$
hydrostatic fluid pressure	p
identity matrix	$\mathbf{I}$
chemical expansion stress	T_c
elastic part of the solid matrix stress	σ^{e}
Lamé coefficients of the solid matrix	$\lambda_{\mathrm{s}}, \mu_{\mathrm{s}}$
dilatation	e=tr($\mathbf{E}$)
infinitesimal strain tensor of the solid matrix	$\mathbf{E}$
chemical potential of the fluid (water) phase	μ^{w}
universal gas constant	R
absolute temperature	T
osmotic coefficient	ϕ
molar concentration	$\mathrm{c}^{+}, \mathrm{c}^{-}$
material constants	a_0, κ, B_w
true density	ρ_T^s, ρ_T^w
electrochemical potential	$\tilde{\mu}^{+}, \tilde{\mu}^{-}$
molecular weight	$\mathrm{M}_{+}, \mathrm{M}_{-}$
activity coefficients	γ_{+}, γ_{-}
Faraday constant	F_{c}
electrical potential	ψ
fixed charge density (FCD)	c^F
mean activity coefficient of the salt	$\gamma_{\pm} = \sqrt{\gamma_{+}\gamma_{-}}$
mean activity coefficient in external solutions	$\gamma_{\pm}^{*}$
modified chemical potential functions	$\varepsilon^{\mathrm{w}}, \varepsilon^{+}, \varepsilon^{-}$
sum of ion concentrations	$c^k = c^{+} + c^{-}$
velocity	$\mathbf{v}^s, \mathbf{v}^w$
material constant	$\alpha = \dfrac{\phi^w}{k}$
hydraulic permeability	k
volume fraction	$\phi^s = \frac{dV^s}{dV}; \phi^w, \phi^{+}, \phi^{-}$
diffusivities	D^{+}, D^{-}

domain	$\Omega^b, \Omega^w, \Omega^s$
displacement of the solid	$\mathbf{u}^s$
Young's modulus of the solid	E
stoichiometric factors	$n_i, i \in \{A, B, C\}$ (A,B,C are chemical substances)
consumption rates of ions	η^+, η^-
functions of ion concentration	r^+, r^-
variables which incorporate molar weights of A and B and the reaction-rate constant	R^+, R^-
concentration-dependent part of the production rate	f
characteristic macroscopic length	L
characteristic microscopic length	ℓ
characteristic microscopic lengths associated with ion diffusion in the pore	$\ell^+ = \sqrt{H_+}\ell, \ell^- = \sqrt{H_-}\ell$
characteristic diffusion times	τ
microscopic time	t
characteristic macroscopic time	$S \pm$
reference concentration	c_0
reference pressure	p_0
surface of discontinuity/interface	Γ

Chapter 1. Introduction

The ever-growing field of non-invasive diagnostic technologies is continually providing new insights into *in vivo* biological processes, requiring joint efforts among researchers in medicine, science, and engineering. One of these emerging technologies, Magnetic Resonance Elastography (MRE), uses an imaging technique to measure the elasticity of biological tissues subject to mechanical stresses.[11, 12] The resulting strains are measured using magnetic resonance imaging and the related elastic modulus is computed from models of tissues mechanics. The elastic modulus contains important information about the pathology of the imaged tissues. Thus, MRE can help in tumor detection, determination of characteristics of disease, and in assessment of rehabilitation.

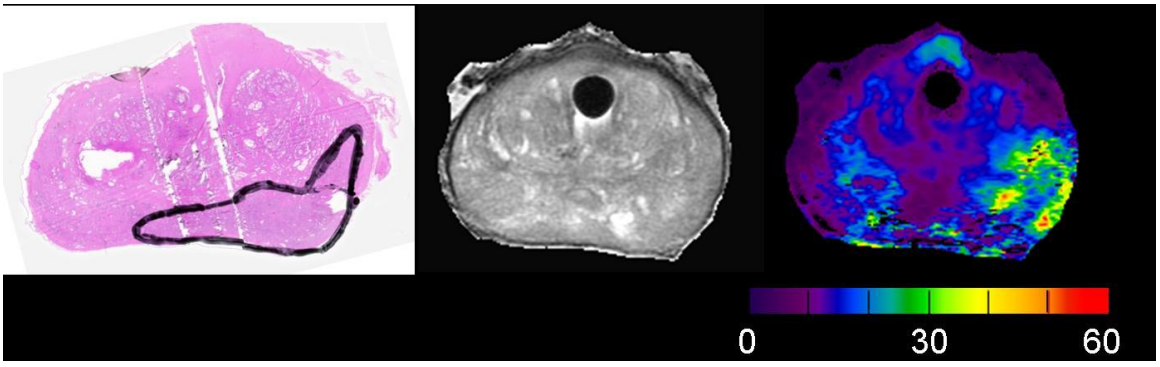

Figure 1.1: Three images of the same malignant tumor in a prostate tissue sample, shown by a) the black outline in a pathology sample, b) MR image, and c) the yellow-red areas in the MR elastogram (MRE Lab, Mayo Clinic)

Figure 1.1 demonstrates the difference between two current diagnostic technologies and MRE, which are all images of the same sample of prostate tissue with a malignant tumor. The first image (a) is a standard pathology sample, while the second image (b) is a Magnetic Resonance image (MRI), and both require a highly trained professional to accurately interpret the results. The third image (c) is an MR elastogram, which clearly demonstrates the location of the tumor, matching the conclusions drawn from the pathology sample. The dark hole in the last two images results from the placement of the actuator, which creates the waves propagating through the tissue needed for MRE. If MRE were used to measure tissue within a living person instead of an *in vitro* tissue sample, the actuator would not be inserted into the person though. For example, if

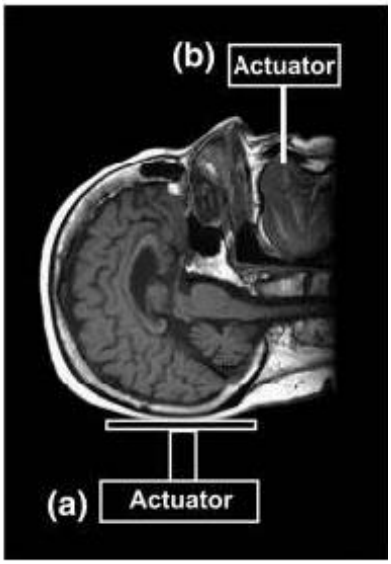

Figure 1.2: Method for creating an elastogram of the brain[9]

MRE were to be used to characterize a person's brain tissue, the actuator would most likely be held between the teeth of the patient, as shown in Figure 1.2(b). Another possible location of an actuator is shown in Figure 1.2(a) but has been demonstrated to be inviable due to disconfort to the patient.

It was noticed experimentally that most biological tissues have incompressible viscoelastic features: they have a certain amount of rigidity that is characteristic of solid bodies, but, at the same time, they flow and dissipate energy by frictional losses as viscous fluids do.[4, 6] The incompressibility assumption for soft tissues is based on the fact that most tissues are made primarily of water. In addition, since the displacements in MRE are very small (on the order of microns), a linear constitutive law is usually assumed. However, despite the richness of the data set, the variety of processing techniques and the simplifications made in the biomechanical model, it remains a challenge to extract accurate results at high resolution in complex, heterogeneous tissues from the intrinsically noisy data. Therefore, any improvement in the MRE data processing with the help of biomechanics and computational methods will be of significant importance to modern medicine.

The aim of this thesis is to formulate a new mathematical model that will be able to differentiate not only between normal and abnormal tissues, but, more importantly, between benign (not cancerous) and malignant (cancerous) tumors. As will be discussed in Section 2.5, benign tumors are localized, self-contained (encapsulated), with smooth boundaries, and tend to be more isotropic. On the other hand, malignant tumors are not localized, diffuse, have irregular boundaries, and are anisotropic. In a recent study by Drapaca and Palocaren[3], MRE data demonstrated a difference in stiffness between a high-grade and low-grade glioma: the high-grade glioma was characterized by a much higher stiffness than the low-grade glioma, which in turn was much stiffer than healthy

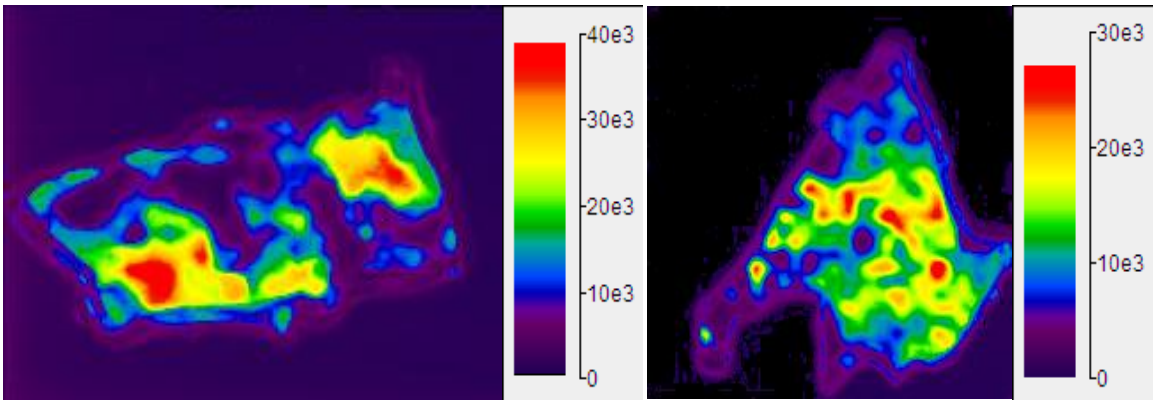

Figure 1.3: MR elastograms comparing a) a high-grade and b) a low-grade glioma. Note that the scale in (a) is from 0-40kPa and in (b) from 0-30kPa. The highest stiffness in the healthy tissue is approximately 12 kPa.[3]

tissue (Figure 1.3). This supports the possibility of using MRE data for both non-invasive detection and characterization of tumors.

The biomechanical models used so far in MRE are classic macroscopic models that do not incorporate any relevant information about the biochemical and mechanical processes that take place in tissue's microstructure and thus fail to properly classify tissues according to their pathology. This thesis involved designing a novel multiscale model that has the potential to differentiate not only between healthy and diseased tissues but also between benign and malignant tumors. The tissue is modeled as a triphasic material of porous, viscoelastic solid filled with interstitial fluid and dissolved ions.[7,17] A recently-developed homogenization technique for materials with evolving microstructure was used in the model,[13,14,15] and the model was implemented for a simple case.

The thesis is structured as follows. In chapter 2 we present a brief review of the literature, covering concepts of continuum mechanics, constitutive theory, thermodynamics, multiscaling, and biology. In chapter 3 we introduce our model and preliminary results are presented in chapter 4. The thesis ends with a chapter of conclusions and future work.

Chapter 2. Review of Literature

2.1 Definitions

Before describing the concepts and equations involved in the triphasic model, certain terms need to be defined. Stress (σ) refers to the magnitude of an applied force per unit area. Strain (ε) is the degree of deformation of an object relative to its original configuration. Deformation is the transformation of an object from a reference configuration into a new one, whether by a lengthening, a shortening, or a more complicated changing of its shape. A deformation gradient ($F = \left(\frac{\partial x^k}{\partial X^k}\right)$, where x^k and X^k are components of the position vector of a point in the deformed and reference configurations, respectively) in an object describes the change in shape throughout the body of the object when subject to deformation. The Jacobian of deformation ($\mathcal{J} = det\left(\frac{\partial x^k}{\partial X^k}\right)$) refers to the volume change associated with deformation of the object. If the object under consideration is incompressible, no volume change can occur, and the Jacobian of deformation equals one. A continuous medium is a material which can be described by continuous functions, because it completely fills the region it occupies without gaps. When solving problems related to continuous media, the mathematical framework called continuum mechanics is applied. In continuum mechanics, from a given deformation of an object, equations of kinematics can be applied to find the strain, from which the stress can be calculated through constitutive equations, and finally, information about the external loading can be obtained from the stress through the equations of motion. This thesis was concerned with defining constitutive relationships between the stress and strain for brain tissue. Because this model incorporates fluid, solid, and ion phases, ion transport needed to be studied, in addition to the mechanical relationship between the fluid and solid. One of the key terms associated with ion transport is the electrochemical potential ($\tilde{\mu}_i$), which describes the effects of electric fields and ion concentration on the motion of that particular ion species.

2.2 Kinematics in Continuum Mechanics

The first topic that must be discussed to properly explain the model under study is kinematics, the study of the motion of objects and systems. Through kinematics, the deformation of a material can be described as strain. When designing this model for biological tissue, it was necessary to understand deformation in order to be able to relate deformation at the microscopic level to deformation at the macroscopic level. The relationship between microscopic structures and macroscopic behavior will be discussed in more detail in later sections. The main concepts in kinematics that need to be understood are the Axiom of Continuity, Law of Motion, and the Laws of Conservation.

2.2.1 Axiom of Continuity

The axiom of continuity (also known as the Archimedean axiom) formally defines continuity, which is important in considering continuous materials such as biological tissue. The definition is as follows: given two points A and B on a straight line, there exists a point A_1 between A and B. On the line AB, there also exist a finite number of points A_2, A_3, … A_n, where A_2 lies between points A_1 and A_3, A_3 lies between points A_2 and A_4, and so on. The line segments AA_1, A_1A_2, … $A_{n-1}A_n$ are all of equal length. Therefore, there must exist a point A_n in the series of points A_1, A_2, … A_n where point B lies between point A and point A_n.[8] The axiom of continuity gives rise to two important concepts: impenetrability and indestructibility of matter. The theory of the impenetrability of matter states that one section of matter can never penetrate into another.[2] Consequently, in relation to deformation, two different points P_1 and P_2 located in a continuous material in its reference configuration cannot occupy the same point P_3 in a deformed configuration of the material. According to the theory of the indestructibility of matter, a region of finite volume cannot be deformed into a region either without volume or of infinite volume.[2] However, the axiom of continuity is not valid for multiphase materials, such as biological tissues.

2.2.2 Law of Motion

The second main concept to consider in kinematics is the Law of Motion. Consider a continuous medium that undergoes a deformation. It occupies the open, bounded, and connected region Ω in its reference configuration at time t = 0 and a different open, bounded, and connected region Ω_t in its deformed configuration at some time t > 0. If there is a point P in the continuous medium, then let its position vector in the reference configuration be $\vec{X} = (X^1, X^2, X^3)$ at t = 0, and let its position vector in the deformed configuration be $\vec{x} = (x^1, x^2, x^3)$ at t >0. According to the law of motion, the deformed position vector $\vec{x}$ must be a function of the reference position vector and time, i.e. $x^i = f_i(X^1, X^2, X^3, t)$, $\forall$ t > 0.[2] Each component of the deformed position vector is a function of time and all components of the reference position vector.

2.2.3 Laws of Conservation

According to the laws of conservation, there are four physical properties that must be conserved during the deformation of a continuous material: mass, linear momentum, angular momentum, and energy. The rate of change of one of these physical properties φ in a specific volume Ω_t over time must equal the internal source of φ plus the flux of φ through the boundaries of Ω_t. There are two ways of writing this mathematically. Conservation can be considered at a global level, which is the "weak" form of the law of conservation, through the equation:

$$\frac{\partial}{\partial t}\int_{\Omega_t}^{i}\varphi(\vec{x},t)dV_t = \int_{\Omega_t}^{i}s(\varphi)dV_t - \int_{\partial\Omega_t}^{i}\vec{f}(\varphi)\cdot\vec{n}dA_t \tag{2.2.1}$$

where $\partial\Omega_t$ refers to the region's boundary, dV_t and dA_t are differential elements of volume and area in the deformed configuration, $\vec{f}$ is the flux, $\vec{n}$ is the unit outer normal to the region boundary, and $s(\varphi)$ is the internal source of the physical property φ. This form is considered "weak" because it is written in integral form. At the local level, the differentiability of φ can be assumed, and the equation can therefore be written in its "strong" form:

$$\frac{\partial\varphi}{\partial t} = s(\varphi) - \nabla\cdot\vec{f}(\varphi) \tag{2.2.2}$$

where the material is in the Ω_t or deformed configuration. From this equation come the local forms of the conservation laws. Assuming there are no internal sources of mass, the law of conservation of mass becomes the equation of continuity in global and local forms,

$$\frac{\partial}{\partial t}\int_{\Omega_t}^{i}\rho dV_t = \int_{\Omega_t}^{i}s(\varphi)dV_t - \int_{\partial\Omega_t}^{i}(\rho\vec{v})\cdot\vec{n}dA_t \tag{2.2.3}$$

$$\frac{\partial\rho}{\partial t} + \nabla\cdot(\rho\vec{v}) = 0 \tag{2.2.4}$$

where ρ is the density in the deformed configuration. In the reference configuration, $\rho_0 = \rho\mathcal{J}$, where $\mathcal{J}$ is the Jacobian of deformation.

The law of conservation of linear momentum, which is in fact Newton's second law of motion for a continuum, becomes the equation of motion in its global and local forms:

$$\frac{\partial}{\partial t}\int_{\Omega_t}^{i}\rho\vec{v}dV_t = \int_{\Omega_t}^{i}\vec{b}dV_t + \int_{\partial\Omega_t}^{i}\vec{t}dA_t \tag{2.2.5}$$

where $\int_{\Omega_t}^{i}\vec{b}dV_t$ accounts for the body forces on the material and $\vec{t}$ is the stress vector resulting from external surface forces, and, respectively:

$$\frac{\partial}{\partial t}(\rho\vec{v}) = \vec{b} + \nabla\cdot\mathbb{T} \tag{2.2.6}$$

where $\mathbb{T}$ is the Cauchy stress tensor, defined by Cauchy's Theorem. Cauchy's Theorem states that the stress vector $\vec{t}$ acting on one side of a surface element is equal and opposite to the stress tensor acting on the other side of that surface element.[2] The Cauchy stress tensor is defined as $\mathbb{T}(\vec{x},t)\vec{n} = \vec{t}(\vec{x},t,\vec{n})$. Equation (2.2.6) is known as the Cauchy equation of motion.[2]

The law of conservation of energy states that the rate of change of energy over time equals the sum of the work done by body forces and surface forces, minus the energy lost through heat flux. For example, in global form, the total energy equation is:

$$\frac{\partial}{\partial t}\int_{\Omega_t}^{i}(W+\frac{1}{2}\rho\vec{v}^2)dV_t = \int_{\Omega_t}^{i}\vec{b}\cdot\vec{v}dV_t + \int_{\partial\Omega_t}^{i}(\mathbb{T}\vec{n}\cdot\vec{v})dS_t - \int_{\Omega_t}^{i}\vec{h}\cdot\vec{n}dA_t \quad (2.2.7)$$

where W is the energy density, dS_t is the differential surface element in the deformed configuration, and $\vec{h}$ is the heat flux vector.

2.3 Constitutive Theory

Standard equations of state have been established for general groups of materials, such as Hooke's Law for linear elastic materials. There are two types of constitutive laws: 1) microstructural and 2) phenomenological equations. Microstructural or rheological equations were derived from principles of physics and the individual measurements of the material's microstructural components. The equations were then derived based on the theoretical interactions between the microstructural components and multi-scaling techniques used to derive a macroscopic model.[2] One example of this type is Fick's law of diffusion. Phenomenological equations were derived from fitting stress-strain curves to experimental data and taking the microstructure of the material into account.[2] An example of this type is Darcy's law.

2.3.1 Linear Elastic Materials

One of the most basic constitutive models for a material is Hooke's Law for linear elastic materials. This law relates stress and strain by

$$\sigma^{ij} = C^{ijkl}\varepsilon_{kl} \quad (2.3.1)$$

where σ^{ij} is the linearized Cauchy stress tensor, ε_{kl} is the infinitesimal strain tensor, and C^{ijkl} is a tensor of elastic moduli independent of stress and strain.[1,2] If this linear elastic solid is also isotropic and homogeneous, then equation (2.3.1) becomes:

$$\sigma^{ij} = \lambda\varepsilon_{\alpha\alpha}\delta^{ij} + 2\mu\varepsilon_{ij} \quad (2.3.2)$$

where λ and μ are the independent Lamé coefficients dependent on the properties of the material.[1,2] They are related to Young's modulus (E) and Poisson's ratio (ν) by the following equations:

$$\frac{E}{2(1+\nu)} = \mu \quad (2.3.3)$$

$$\frac{E}{3(1-2\nu)} = 2\mu + 3\lambda \quad (2.3.4)$$

Young's modulus is associated with the stiffness of a material and is the ratio between the uniaxial stress on a material and the degree of its axial deformation (Greenleaf).[1] Poisson's ratio describes the relationship between the lengthening of a material and the narrowing of its width under stress. Mathematically, Poisson's ratio is the ratio between the transverse strain and the axial strain. The Lamé coefficient μ is also called the shear modulus of the material, which is the ratio between transverse strain and transverse stress (Greenleaf).[2] It denotes the material's resistance to shear stress.[1]

2.3.2 Hyperelastic Solids

The second basic constitutive law is the Mooney-Rivlin law for non-linear elastic or hyperelastic solids. It describes the dependence of the stress tensor on the material's deformation gradient F with the equation

$$T = \mathcal{J}\frac{\delta W(F)}{\delta F}F^T \tag{2.3.5}$$

where $\mathcal{J} = \left|\frac{\delta x^k}{\delta X^k}\right|$ is the Jacobian of deformation and W is the internal density function defining the material's internal energy as $\int_{\Omega_t}^{l} W dv$.[2] Ω_t is the domain of the deformed configuration of the material.

2.3.3 Non-Newtonian Fluids

The third constitutive equation deals with fluids instead of solids: the Reiner-Rivlin constitutive equation for an isotropic non-Newtonian fluid. The general form follows the equation

$$T = \mathcal{F}(L, \rho, \vec{x}) \tag{2.3.6}$$

where $L = \left(\frac{\delta x^k}{\delta x^j}\right)_{j,k=\overline{1,3}}$ is the velocity gradient tensor and ρ is the fluid mass density.[2] Because the stress tensor T is a linear function, it can be written as a polynomial using the Taylor series expansion.

2.3.4 Viscoelastic Materials

Viscoelastic materials are those which have characteristics normally associated with solids as well as those normally associated with liquids. Because of their hybrid nature, the wide variety of viscoelastic materials fills the spectrum between solids and fluids. They are the class of material most relevant to biological tissues. Four of the most basic models for viscoelastic materials are discussed in this section: (1) the Maxwell model, (2) the Kelvin-Voigt model, (3) the standard linear model, and (4) the quasi-viscoelastic constitutive model.

The first three models mentioned before are microstructural or rheological models, based on theoretical arrangements of linear springs and non-linear dashpots. The Maxwell model is based on a perfectly elastic spring and a perfectly viscous dashpot in series (Fig. 2.3.1).

Figure 2.3.1: Maxwell model of a viscoelastic material

If a sudden force F_0 were applied and held, the spring would lengthen instantly according to the simplified version of Hooke's Law in 1D:

$$F_0 = kx \tag{2.3.7}$$

where k is the spring constant and x is the change in length of the spring. The dashpot, being a perfectly viscous damping element, would linearly increase its length over time, according to the Newtonian case of the Reiner-Rivlin constitutive equation in 1D:

$$F_0 = \mu\dot{x} \tag{2.3.8}$$

where μ is the viscosity and $\dot{x}$ is the rate of change in length of the dashpot over time.[1,2] A Maxwell material therefore undergoes the process of creep under a constant force. If the force were released, the spring would return to its original length, but the dashpot would not. Therefore, after a force were applied and released, the system's final length would be between its original length and the length reached under the applied force. Continued deformation after an applied stress is released is characteristic of a fluid. Maxwell materials are therefore considered more fluid than solid.

If the Maxwell model were exposed to a sudden, constant deformation instead of a constant force, the viscous element would slowly relieve the stress on the elastic element. This process is called stress relaxation.[2]

The Kelvin-Voigt model describes materials who behave similarly to a perfectly elastic spring and a perfectly viscous dashpot in series (Fig. 2.3.2).

Figure 2.3.2: Kelvin-Voigt model of a viscoelastic material

Because the dashpot and the spring are in series, if a sudden force were applied, the spring would not be able to immediately stretch to the full displacement described by equation 10. The displacement of the spring must equal the displacement of the dashpot.

As the dashpot lengthens, the displacement of the system approaches the spring's full displacement. After that has been reached, the spring prevents the system from lengthening further.[1,2] When the force is released, the system returns to its original length over a period of time dependent on the dashpot's viscosity. Returning to the original configuration after an applied stress is released is a characteristic of a solid, which means that Kelvin-Voigt materials are considered more solid than fluid.[2]

The standard linear model is a combination of the Maxwell and the Kelvin-Voigt models (Fig. 2.3.3).

Figure 2.3.3: Standard linear model of a viscoelastic material

This type of viscoelastic material acts like a solid at the instant a force is applied, as in the Maxwell model, and like a solid, it reaches a maximum displacement, as in the Kelvin-Voigt model. In between those times, it acts more like a liquid due to the viscous element's influence.[1]

The fourth model for viscoelastic materials is a phenomenological model, representing viscoelastic behavior through integral representation.[2] The quasi-linear viscoelastic constitutive model proposed by Fung is based on Hooke's Law for elastic materials, where:

$$\sigma^{(e)} = C\varepsilon^{(e)}. \tag{2.3.9}$$

The elastic stress rate $\dot{\sigma}^{(e)}$ is therefore related to the elastic strain rate $\dot{\varepsilon}^{(e)}$ by:

$$\dot{\sigma}^{(e)} = C\dot{\varepsilon}^{(e)}. \tag{2.3.10}$$

For linear viscoelastic materials, the viscoelastic stress is proportional to the viscoelastic strain rate, not the strain itself. According to Fung's model:

$$\sigma^{(ve)} = G' * \dot{\varepsilon}^{(ve)} \tag{2.3.11}$$

where $*$ is the convolution operator, such that:

$$G' * \dot{\varepsilon}^{(ve)} = \int_0^t G'(t-\tau)\,\dot{\varepsilon}(\tau)d\tau \tag{2.3.12}$$

and $G'(t-\tau)$ represents the fluid characteristics of the viscoelastic material and $\dot{\varepsilon}(\tau)$ represents the solid characteristics. Because $\dot{\varepsilon}(\tau)$ is not time-dependent, it can be approximated as the elastic strain rate:

$$\sigma^{(ve)} = G' * \dot{\varepsilon}^{(e)} \tag{2.3.13}$$

which is why this model is called quasi-linear. Combining equations (2.3.10) and (2.3.13), equation (2.3.13) becomes:

$$\sigma^{(ve)} = G * \dot{\sigma}^{(e)} \tag{2.3.14}$$

so that it is completely dependent on the material's stress and stress rate.[2] G is the result of combining the terms G' and C from equations (2.3.10) and (2.3.13), respectively.

2.3.5 Rules for Constitutive Equations

From a mathematical point of view, when determining the constitutive equations for a material, the following general principles must be adhered to: (1) coordinate invariance, (2) the principles of determinism and local action, (3) equipresence, and (4) material frame indifference. If not, the resulting equations would not be dependent on the inherent characteristics of the material of interest and could not therefore be termed "constitutive."

A coordinate system which is used to describe an object does not affect that object's motion or deformation in any way. Therefore, constitutive equations modeling the object's behavior must also not depend on the coordinate system[19]. This is the principle of coordinate invariance. Tensors, which are linear functions of vectors, are geometrically invariant, which means they are unaffected by changes in coordinate systems.[2] This makes tensor form ideal for constitutive equations [19].

For a viscoelastic material such as tissue, the principle of determinism states that deformation results in energy loss specific to the path taken from the old to the new configuration[19]. This path dependence means that every deformation of a body affects the stress state within the body, both during the deformation and after it has occurred. This property is known as the "memory" of the material.[2] However, for a given point $\vec{x}$ in a body, only the deformation history of an arbitrarily small neighborhood of $\vec{x}$ affects the stress at $\vec{x}$, according to the principle of local action. Therefore, the stress present at a point $\vec{x}$ in a body at time t > 0 is dependent not only on the instantaneous deformation and temperature, but also on the deformation history of the arbitrarily small neighborhood around it [19]. This principle takes the form of the equation:

$$T(\vec{x}, t) = \mathcal{F}\left(\vec{x}^{t}; \vec{X}, t\right) \tag{2.3.15}$$

where T is the stress tensor, $\mathcal{F}$ is the constitutive operator, $\vec{x}$ is the position vector in the Eulerian coordinate system, $\vec{X}$ is the position vector in the Lagrangian coordinate system, and $\vec{x}^{t}$ is the material "memory" of deformation.[2]

According to the principle of equipresence, for a given material, each independent variable which is taken into account must be incorporated into every constitutive equation for that material, as long as the other constitutive principles are upheld [19].

The last principle of material frame indifference states that any motion of an observer with respect to a point $\vec{x}$ in a body does not affect any motion or deformation occurring at $\vec{x}$. Therefore, the constitutive equations for a body must be independent of the observer's frame of reference, or "frame-indifferent"[19].

Certain assumptions need to be made when considering constitutional models, so that the associated equations are more easily solved. The first is to assume that a given material is a simple one. Within an arbitrarily small neighborhood of a given point $\vec{x}$ in a simple material, only the effects of the independent variables and their first derivatives are significant enough to be considered[19.] This gives a constitutive equation of the form:

$$T(\vec{x},t) = \mathcal{F}(F^t(\vec{X},s);\vec{X},t) \tag{2.3.16}$$

where $F^t(\vec{X},s) = F(\vec{X},t-s), \forall s \in [0,\infty)$ is F's material history until time = t.[2]

A second assumption is that the material under consideration is homogeneous.[2] For biological materials, this is rarely true, but with careful application of multiscaling, a homogeneous approximation of tissue could be calculated. For a homogeneous material, the constitutive equation becomes[2]:

$$T(\vec{x},t) = \mathcal{F}(F(\vec{x},t)) \tag{2.3.17}$$

Another common assumption is that a material is non-aging which means that changes at microscopic level can be neglected, but for obvious reasons, this assumption cannot be applied to biological tissue. Thus a constitutive equation of the form:

$$T(\vec{x},t) = \mathcal{F}(F^t(\vec{X},s);\vec{X}) \tag{2.3.18}$$

is usually employed for an aging, simple material.[2]

A third simplifying assumption that cannot be directly applied to a biological material is that it is isotropic. The properties of an isotropic material are the same in all directions. For example, if there is a sphere of isotropic material, its response to an applied normal force would not change because of the direction of the applied force. An anisotropic material does not respond equally to applied forces of equal magnitude in any direction. One example of this type of material is graphite, which has strong bonds within each layer of carbon and much weaker bonds holding the layers together.

A last set of assumptions that can be applied are simplifying constraints on the internal material properties, such as inextensibility, rigidity, and incompressibility.[2]

Inextensibility and rigidity do not apply to soft biological tissues, which are viscoelastic and can therefore be deformed under stress. The liquid phase of tissue is primarily water, however, which can be assumed to be incompressible.

2.4 Thermodynamics

The primary application of thermodynamics to this model relates to equilibrium thermodynamics and the transport processes. The transport of ions across cell membranes is very important to cell function and can be affected by pathological conditions, such as cancer. The main driving force behind transport across membranes is the electrochemical gradient.

2.4.1 Chemical and Electrochemical Potentials

The electrochemical potential is dependent on the composition of the solution under study, the pressure, and the temperature.[5] The equation for electrochemical potential can be defined as:

$$\tilde{\mu}_i = \bar{V}_i P + RT \ln c_i + z_i \mathfrak{F} \psi + \mu_i^0 \tag{2.4.1}$$

where $\tilde{\mu}_i$ is the electrochemical potential of the *i*th species of ionic solute. In the first term, $\bar{V}_i$ is the partial molar volume of the *i*th species, and P is the pressure. In the second term, R is the universal gas constant, T is the absolute temperature, and c_i is the concentration of the *i*th species. In the third term, z_i is the valence of the *i*th species, $\mathfrak{F}$ is the Faraday, and ψ is the electrostatic potential. The last term, μ_i^0, is the chemical potential at a defined standard concentration, usually 1 mol/L.[5] A similar equation is defined for the chemical potential μ_i:

$$\mu_i = \bar{V}_i P + RT \ln c_i + \mu_i^0 \tag{2.4.2}$$

where the third term of equation (2.4.1) is removed.

Because equations (2.4.1) and (2.4.2) are based on dilute solutions, which are much lower than concentrations evident in biological fluids, an adjustment to the equations must be made. To be able to accommodate higher concentrations, solute concentration c_i is replaced with the solute activity a_i, which is usually determined experimentally through the relation[5]:

$$\mu_i = \bar{V}_i P + RT \ln a_i + \mu_i^0 \tag{2.4.3}$$

In dilute solutions, a solute particle can be assumed to never encounter or interact with other solute particles. Substituting a_i into equations (2.4.1) and (2.4.2) accounts for the effects of solute-solute interactions in concentrations found in physiological conditions. The relationship between the solute activity and concentration is:

$$\gamma_i = \frac{a_i}{c_i} \tag{2.4.4}$$

where γ_i is the activity coefficient of the *i*th species of solute. Under physiological conditions, the interactions of interest between solute particles are primarily electrostatic.[5] Accordingly, only the activity coefficients of charged solute particles are considered to be other than unity.

2.4.2 Electrostatic Interactions

There are two main types of electrostatic interaction. The first kind involves the effect of a charged solute particle's electric field on another solute particle or on the localized region of solvent around the particle. The main theory dealing with this type of interaction is the Debye-Hückel theory, which states that the activity coefficient of a charged solute particle is dependent on the ionic strength *Z* of a solution, where:

$$Z = \frac{\sum z_i^2 c_i}{2} \tag{2.4.5}$$

and z_i is the charge number of the *i*th species of solute ion. The interactions between ions at biological concentrations cause γ_i to be continually less than one.[5]

The second type of electrostatic interaction is the binding of a charged solute particle to another solute or to an insoluble particle. If ion-ion interactions are relatively insignificant compared to the effects of solute binding, then the activity coefficient can be approximated as the fraction of unbound solute.

Several kinds of biological solutes involve multiple charges distributed along the length of their structures, such as proteins and certain polysaccharides. These involve a combination of the two types of electrostatic interaction. They can interact with small ions in a manner similar to that described by the Debye-Hückel theory, but their multiple charges can create "cooperative effects" which behave in a manner more closely related to ion binding.[5] Such complex interactions mean that the activity coefficient cannot be predicted. To overcome this difficulty, the concentration can be used in place of the solute activity, as long as the activity coefficient is uniform. This is because in characterizing the transport rate, the gradient of the chemical potential is more important than the potential itself.[5] To demonstrate the feasibility of replacing a_i with c_i, the derivative is taken of the second term of equation (2.4.3):

$$d(RT \ln a_i) = RT \frac{da_i}{a_i} = RT \left(\frac{dc_i}{c_i} + \frac{d\gamma_i}{\gamma_i} \right) \tag{2.4.5}$$

where if γ_i is uniform, then $d\gamma_i$ = 0, and consequently, it is proved that c_i can successfully replace a_i in an equation for the chemical potential gradient.

2.4.3 Physiological Conditions

In this case the only solute particles which will be considered are ions. Ions comprise an overwhelming majority of the solutes dissolved in biological fluids, and most of those are monovalent.[5] Therefore, the molar concentration of ions can be used to approximately equal a biological solution's ionic strength. Throughout the fluid phases in the human body, the ionic strength is nearly the same, despite the differences in ionic composition.[5] Because the activity coefficient is dependent on the ionic strength, bodily fluids' activity coefficients can be approximated to be the uniform among the different biological fluids, as well. As previously stated, if the activity coefficient is uniform, the concentration of the *i*th species can be used instead of solute activity, so in this sense, biological properties simplify the equation for chemical potential

However, as previously mentioned, there does exist ion binding in biological fluids, which lessens the accuracy of the assumption that the activity coefficient is uniform in bodily fluids. Concentration measurements frequently do not distinguish between bound and unbound ionic particles, which affect the estimation of the activity coefficient. In order to simplify this problem, the ions can be modeled as two separate groups, bound and unbound, where γ_{bound} is assumed to be zero and γ_{free} is approximately one. This representation enables the replacement of the total solute activity by the concentration of the unbound ions.

2.5 Biology

Although our model is only a first step toward characterizing the differences between benign and malignant tissues, and most of the complex biology is not considered, the aim of this research is to eventually provide a model of brain tissue for cancer diagnosis with MRE. Therefore, an overview of brain tissue physiology and malignant and benign tumors will be discussed.

2.5.1 Brain Tissue

Brain tissue is composed of two distinct types of tissue: gray matter and white matter, as can be seen in Figure 2.5.1. Gray matter and white matter have very different cellular compositions. White matter is composed primarily of the myelinated axons of neurons. A myelinated axon is one which is covered with a myelin sheath. These myelin sheaths are formed by cells called oligodendrocytes wrapping extensions of their cell

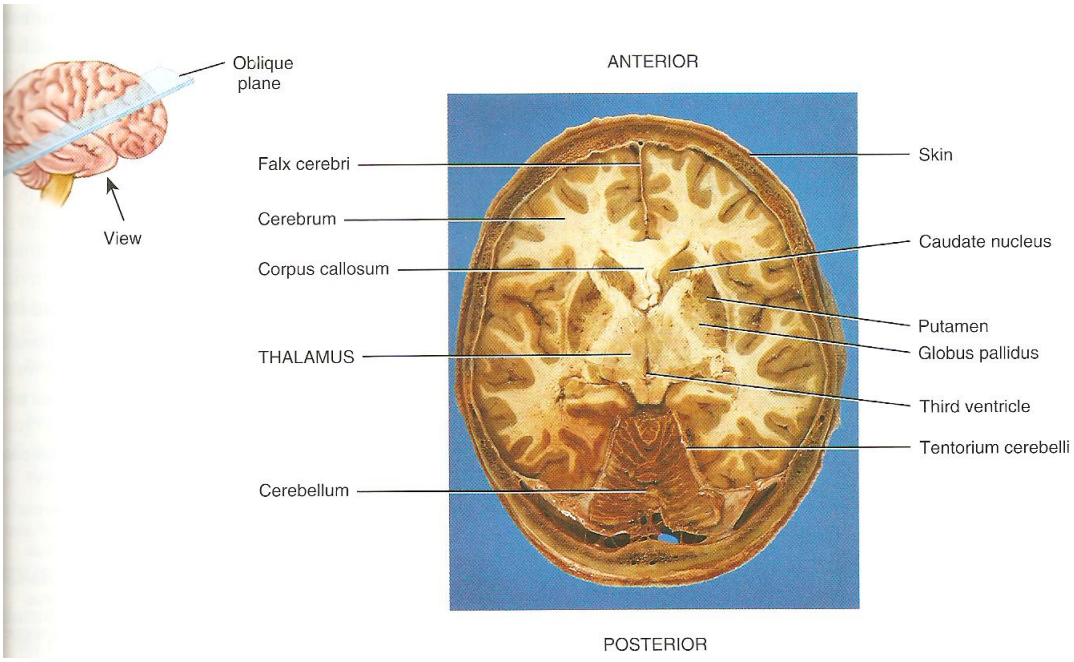

Figure 2.5.1: Oblique section of the human brain; darker areas are gray matter and lighter areas are white matter[18]

membranes around the axon of a neuron, forming several layers of protective membrane (Figure 2.5.2). This increases the velocity of the neuronal signal as it is transmitted along the neuron. There are small exposed spaces between lengths of myelin sheath along the axon called the nodes of Ranvier, and the signal must "jump" from one node to the next.

Gray matter has a much more complicated composition and contains the various types of brain cells called neuroglia shown in Figure 2.5.2. One cell worthy of specific mention is the fibrous astrocyte, which is one of the cells forming part of the blood-brain barrier. The blood-brain barrier keeps most substances in the bloodstream from entering the cerebrospinal fluid and interacting with the neuronal cells in the brain. The fibrous astrocyte wraps extensions of its cell membrane around blood vessels in the brain, forming a protective barrier between it and the surrounding cerebrospinal fluid.[18] Because gray matter consists of all of these different types of cells, it is more densely packed and therefore stiffer than white matter. This inherent heterogeneity of brain tissue will have to be taken into account in future work on modeling brain tissue.

2.5.2 Cancer Physiology

The main thrust of this thesis is that benign and cancerous tumors will be able to be detected and differentiated non-invasively through Magnetic Resonance Elastography. This approach is based on the distinct physiological differences that exist between healthy tissue, benign tumors, and malignant tumors. In the case of a benign tumor, it is formed of cells encapsulated in fibrous tissue, which is stiffer than the healthy cells around it. The capsule is shown in Figure 2.5.3 as the orange band around the benign

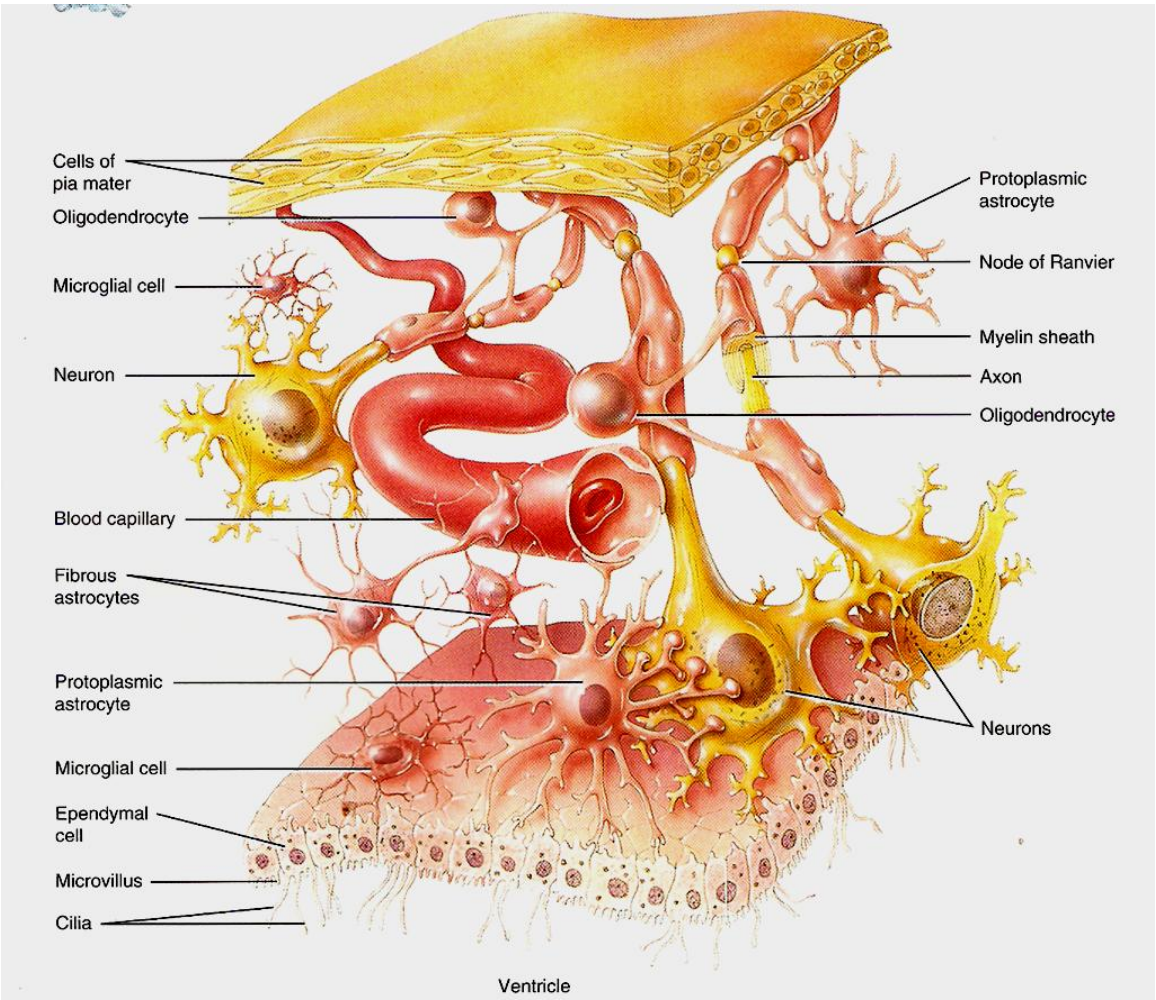

Figure 2.5.2: Neuroglia of the central nervous system[18]

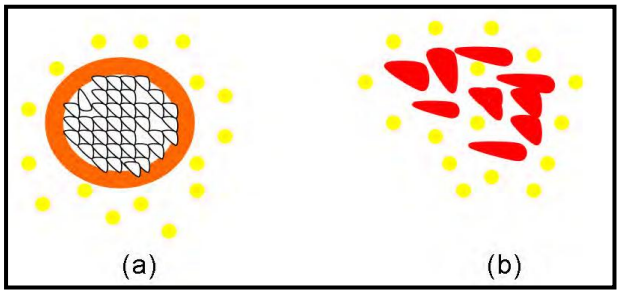

Figure 2.5.3: A diagram showing organizational differences between (a) benign tumors and (b) malignant tumors. Surrounding healthy cells are shown in yellow.[3]

tumor cells. Benign cells are localized to the area of tissue in which the tumor formed and do not spread. When cells turn malignant, they are no longer encapsulated and can metastasize and spread throughout the body. Malignant cells are more diffuse than benign cells and are irregularly shaped, as shown in Figure 2.5.3. It is theorized that the changes in the cell which leads to this conformational change cause the higher stiffness in malignant then benign tumors, which was demonstrated in gliomas through MRE in the study by Drapaca and Palocaren (see Figure 1.3).[3] When a tumor becomes malignant, it also begins angiogenesis, or the formation of blood vessels, to supply it with nutrients. This difference between benign and malignant tumors may be taken into account through modeling the differences in ion transport between the two types of tumors, as discussed later. These differences in characteristics support the theory that modeling healthy tissue, benign tumors, and malignant tumors will enable the use of a non-invasive technique like MRE to detect and diagnose cancer.

2.6 Multiscaling Method

In order to connect microstructural properties to macroscopic behavior, a standard multiscaling method was used. Because biological tissue is typically anisotropic and always evolving, the problem must be simplified in order to mathematically approximate it. In this method, the evolving microstructure is assumed to have undergone a transformation into a periodic microstructure, which is much simpler to model. A periodic macrostructure modeled as an average of repeating microscopic units can then be approximated through a homogenization technique. After this periodic macrostructure has been found, the evolving macrostructure can be approximated by performing a back-transformation. The back-transformation essentially undoes the original transformation which turned the evolving microstructure to periodic.[13] The specific multiscaling method used in this model was outlined by Peter & Böhm[15] and will be described in greater detail in Chapter 3. They proposed a homogenization technique as part of the multiscaling method which deals with domains of evolving microstructure, like biological tissue, which is made of microscopic cells and structures that are continuously changing, growing, and evolving.

Chapter 3. Design of the Tri-Phasic Model

3.1 Tri-phasic Theory

In our study the tissue is assumed to be a porous viscoelastic solid filled with fluid and ion phases. Because of the inclusion of all three phases in the model, our model falls under tri-phasic theory, which has been studied to some extent already. There are a set of standard constitutive equations for tri-phasic materials, as written by Sun et al.[17] upon which part of the model designed in this thesis is based:

$$\boldsymbol{\sigma} = -p\mathbf{I} - T_{\mathrm{c}}\mathbf{I} + \sigma^{\mathrm{e}} = -p\mathbf{I} - T_{\mathrm{c}}\mathbf{I} + \lambda_{\mathrm{s}} e\mathbf{I} + 2\mu_{\mathrm{s}}\mathbf{E} \tag{3.1.1}$$

$$\mu^{\mathrm{w}} = \mu_0^{\mathrm{w}} + [p - RT\phi(\mathrm{c}^+ + \mathrm{c}^-) + B_{\mathrm{w}} e]/\rho_{\mathrm{T}}^{\mathrm{w}} \tag{3.1.2}$$

$$\tilde{\mu}^+ = \mu_0^+ + \left(\frac{RT}{M_+}\right)\ln(\gamma_+ c^+) + \frac{F_{\mathrm{c}}\psi}{M_+} \tag{3.1.3}$$

$$\tilde{\mu}^- = \mu_0^- + \left(\frac{RT}{M_-}\right)\ln(\gamma_- c^-) - \frac{F_{\mathrm{c}}\psi}{M_-} \tag{3.1.4}$$

$$T_{\mathrm{c}} = a_0 c^F e^{-\kappa\left(\frac{\gamma_\pm}{\gamma_\pm^*}\right)\sqrt{c^+ c^-}} \tag{3.1.5}$$

where $\boldsymbol{\sigma}$ is the stress of the tri-phasic mixture, μ^{w} is the chemical potential of the liquid, $\tilde{\mu}^+$ and $\tilde{\mu}^-$ are the electrochemical potentials of the ions, and T_{c} is the chemical expansion stress.[17] A complete list of variables can be found on page v, but one variable which requires more explanation is c^F, which is the fixed charge density. In Sun's model and the model described by this thesis, it is assumed there are charges fixed to the solid phase of the material. In biological tissue, cartilage in the extracellular matrix has ions which are so strongly associated with it that their ability to diffuse through the material is much less than the free ions in the ion phase.[17] Therefore, the ions attached to the solid phase can be assumed to be fixed, and the density or concentration of fixed charges always remains the same.

Sun et al.[17] also described an alternative way to describe the tri-phasic model, which are in terms of the strain tensor and chemical potentials:

$$\nabla\cdot(\lambda e\mathbf{I} + 2\mu_s\mathbf{E}) - \nabla(RT\varepsilon^w + RT\phi c^k - B_w e) = 0 \tag{3.1.6}$$

$$\nabla\cdot\mathbf{v}^s - \nabla\cdot\frac{RT}{\alpha}\left[\phi^w\nabla\varepsilon^w + \frac{\phi^w c^+}{\varepsilon^+}\nabla\varepsilon^+ + \frac{\phi^w c^-}{\varepsilon^-}\nabla\varepsilon^-\right] = 0 \tag{3.1.7}$$

$$\nabla\cdot\left\{\begin{array}{c} -\frac{RT}{\alpha}\phi^w c^F\nabla\varepsilon^w - \left[\frac{\phi^w c^+ D^+}{\varepsilon^+} + \frac{RT}{\alpha}\frac{\phi^w (c^+)^2}{\varepsilon^+} - \frac{RT}{\alpha}\frac{\phi^w c^+ c^-}{\varepsilon^+}\right]\nabla\varepsilon^+ \\ + \left[\frac{\phi^w c^- D^-}{\varepsilon^-} + \frac{RT}{\alpha}\frac{\phi^w (c^-)^2}{\varepsilon^-} - \frac{RT}{\alpha}\frac{\phi^w c^+ c^-}{\varepsilon^-}\right]\nabla\varepsilon^- \end{array}\right\} = 0 \tag{3.1.8}$$

$$\frac{\partial(\phi^w c^k)}{\partial \mathrm{t}} - \nabla \cdot \left\{ \begin{array}{c} \frac{RT}{\alpha}\phi^w c^k \nabla \varepsilon^w + \left[\frac{\phi^w c^+ D^+}{\varepsilon^+} + \frac{RT}{\alpha}\frac{\phi^w (c^+)^2}{\varepsilon^+} + \frac{RT}{\alpha}\frac{\phi^w c^+ c^-}{\varepsilon^+}\right]\nabla \varepsilon^+ \\ + \left[\frac{\phi^w c^- D^-}{\varepsilon^-} + \frac{RT}{\alpha}\frac{\phi^w (c^-)^2}{\varepsilon^-} + \frac{RT}{\alpha}\frac{\phi^w c^+ c^-}{\varepsilon^-}\right]\nabla \varepsilon^- \end{array} \right\}$$

$$+\nabla \cdot (\phi^w c^k \mathbf{v}^s) = 0 \tag{3.1.9}$$

where ε^w, ε^+, and ε^- are modified chemical potential functions with units of ion concentration, c^+ and c^- are molar concentrations of ions, and ϕ^w is the volume fraction of the liquid (or water) phase.[17] The total volume of the material is composed of the volume fractions of all the components ($\phi^s + \phi^w + \phi^+ + \phi^- = 1$), but the volume of the ions are so small compared to the solid and liquid phases' volumes that they can be neglected. Therefore, it can be assumed that $\phi^s + \phi^w = 1$.

Assuming that the change in displacement is negative, the reference volume fraction of the solid phase can be written as:

$$\phi_0^s = \phi^s(1 + \frac{\partial u}{\partial x})$$

where ϕ_0^s refers to the volume fraction in the reference configuration and ϕ^s in the deformed configuration. The volume fraction of the liquid phase ϕ^w can then be rewritten as:

$$\phi^w = 1 - \frac{\phi_0^s}{1+\frac{\partial u}{\partial x}} \approx (1 - \phi_0^s) + \phi_0^s \frac{\partial u}{\partial x} \tag{3.1.10}$$

because it is assumed the solid displacement $\frac{\partial u}{\partial x} \ll 1$, so $\frac{\partial^2 u}{\partial x^2}$ can be neglected.

The modified chemical potential functions were defined by Sun et al.[17] as:

$$\varepsilon^w = \frac{p}{RT} - \phi c^k + \frac{B_w}{RT} e \tag{3.1.11}$$

$$\varepsilon^+ = \gamma_+ c^+ exp\left(\frac{F_c \psi}{RT}\right) \tag{3.1.12}$$

$$\varepsilon^- = \gamma_- c^- exp\left(-\frac{F_c \psi}{RT}\right) \tag{3.1.13}$$

where in equation (3.1.11), p is the hydrostatic pressure, R is the universal gas constant, T is absolute temperature, ϕ is the osmotic coefficient, c^k is the sum of ion concentrations ($c^k = c^+ + c^-$), B_w is a material constant, and e is the dilatation related to the infinitesimal strain of the solid matrix $\mathbf{E}$ by $e = tr\mathbf{E}$. In equations (3.1.12) and (3.1.13), γ_+ and γ_- are the activity coefficients of the ions, F_c is the Faraday constant, and ψ is the electrical potential. (For reference, the ion activity coefficients were defined and

discussed in Section 2.4.) The next section will describe the ways these equations are modified to suit our new model.

3.2 Design Process

3.2.1 Assumptions

For our model, several simplifying assumptions were made as a first approximation, to determine the feasibility of future development of more complex models. The focus is on brain tissue, although future models will be tailored more closely to the brain's physiology than this preliminary model.

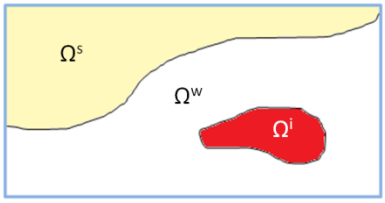

Figure 3.2.1: Diagrams of the three domains in the model: solid, fluid (CSF), and ionic

The model consists of three phases: the solid phase, which represents the cell membranes and the structural proteins in the extracellular matrix in which cells exist; the liquid or water phase, which approximates the aqueous environment of cerebrospinal fluid as pure liquid; and the ion phase, which represents blood. The cerebrospinal fluid and blood are assumed to be incompressible fluids, and the solid phase is assumed to be a linear viscoelastic solid. The tissue is assumed to be locally homogeneous, isotropic, and electroneutral. In order to satisfy the electroneutrality condition, the concentration of positive and negative ions must be equal. Assuming the fixed charges on the solid phase are negative, this means that $c^+ = c^F + c^-$. Therefore, the fixed charge density is defined as the difference between the free cation and anion concentrations:

$$c^F = c^+ - c^- \tag{3.2.1}$$

In addition, there is assumed to be no ion exchange between the cerebrospinal fluid and the blood phases. The blood-brain barrier does prevent many substances in the circulatory system from entering the cerebrospinal fluid, but in reality, there is still ion exchange between the two fluids. However, as previously mentioned, this is intended as a preliminary model, so the ion exchange between the fluids is assumed zero for simplification purposes.

3.2.2 The One-Dimensional Case

The first step of simplifying the equations (3.1.6)-(3.1.9) is to transform them from three dimensions to one dimension. First looking at equation (3.1.6):

$$\nabla \cdot (\lambda e\mathbf{I} + 2\mu_s\mathbf{E}) - \nabla(RT\varepsilon^w + RT\phi c^k - B_w e) = 0 \tag{3.1.6}$$

the first term is equivalent to the gradient of the stress on the solid phase. Changing σ^s from its three-dimensional form:

$$\boldsymbol{\sigma}^s = \lambda_s e\mathbf{I} + 2\mu_s\mathbf{E}$$

to its one-dimensional form:

$$\sigma^s = E\frac{\partial u}{\partial x} \tag{3.2.2}$$

results in the one-dimensional form of Hooke's Law for linear elastic materials. In the last term of (3.1.6), the dilatation $e = tr\mathbf{E}$, becomes in 1D:

$$e = \frac{\partial u}{\partial x}$$

which is the infinitesimal linear displacement of the solid phase in the x-direction. Substituting these into equation (3.1.6) and changing the gradients to partial derivatives with respect to the x-direction gives the following equation:

$$\frac{\partial}{\partial x}\left(E\frac{\partial u}{\partial x}\right) - \frac{\partial}{\partial x}\left(RT\varepsilon^w + RT\phi c^k - B_w\frac{\partial u}{\partial x}\right) = 0$$

which reduces further to:

$$p = E\frac{\partial u}{\partial x} \tag{3.2.3}$$

where we recall that p is the hydrostatic pressure and E is Young's modulus of the solid phase. This is the first constitutive equation of our tissue model.

In order to find the second constitutive equation, equation (3.1.7) must be transformed to one dimension from its three-dimensional form:

$$\nabla\cdot\mathbf{v}^s - \nabla\cdot\frac{RT}{\alpha}\left[\phi^w\nabla\varepsilon^w + \frac{\phi^w c^+}{\varepsilon^+}\nabla\varepsilon^+ + \frac{\phi^w c^-}{\varepsilon^-}\nabla\varepsilon^-\right] = 0 \tag{3.1.7}$$

where $\mathbf{v}^s$ is the velocity of the solid phase, α is a constant related to the hydraulic permeability k by $\alpha = \frac{\phi^w}{k}$, and ϕ^w is the volume fraction of the liquid (water) phase in the tissue. In one dimension, the solid velocity becomes $\mathbf{v}^s = \frac{\partial u}{\partial t}$.

With the assumption that the tissue is electrically neutral ($\psi = 0$), the equations for ε^+ and ε^- are simplified from equations (3.1.12) and (3.1.13):

$$\varepsilon^+ = \gamma_+ c^+ exp\left(\frac{F_c\psi}{RT}\right) \tag{3.1.12}$$

$$\varepsilon^- = \gamma_- c^- exp\left(-\frac{F_c\psi}{RT}\right) \tag{3.1.13}$$

to:

$$\varepsilon^{+} = \gamma_{+} c^{+} \tag{3.2.4}$$

$$\varepsilon^{-} = \gamma_{-} c^{-} \tag{3.2.5}$$

After these simplifications are substituted into equation (3.1.7), this equation becomes in 1D:

$$\frac{\partial}{\partial x}\left(\frac{\partial u}{\partial t}\right) - \frac{RT}{\alpha}\frac{\partial}{\partial x}\left[\phi^{w}\frac{\partial \varepsilon^{w}}{\partial x} + \frac{\phi^{w} c^{+}}{\gamma_{+} c^{+}}\gamma_{+}\frac{\partial c^{+}}{\partial x} + \frac{\phi^{w} c^{-}}{\gamma_{-} c^{-}}\gamma_{-}\frac{\partial c^{-}}{\partial x}\right] = 0$$

which reduces to:

$$\frac{\partial u}{\partial t} = \frac{E + B_{w}}{\alpha}\phi^{w}\frac{\partial^{2} u}{\partial x^{2}} + \frac{RT}{\alpha}\phi^{w}(1-\phi)\frac{\partial c^{k}}{\partial x} \tag{3.2.6}$$

and this is the second constitutive equation for our model, describing the velocity of the solid phase.

Applying these changes to equation (3.1.8), it becomes in 1D:

$$\frac{\partial}{\partial x}\left\{\begin{array}{c} -\frac{RT}{\alpha}\phi^{w} c^{F}\frac{\partial \varepsilon^{w}}{\partial x} - \left[\frac{\phi^{w} c^{+} D^{+}}{\gamma_{+} c^{+}} + \frac{RT}{\alpha}\frac{\phi^{w}(c^{+})^{2}}{\gamma_{+} c^{+}} - \frac{RT}{\alpha}\frac{\phi^{w} c^{+} c^{-}}{\gamma_{+} c^{+}}\right]\gamma_{+}\frac{\partial c^{+}}{\partial x} \\ + \left[\frac{\phi^{w} c^{-} D^{-}}{\gamma_{-} c^{-}} + \frac{RT}{\alpha}\frac{\phi^{w}(c^{-})^{2}}{\gamma_{-} c^{-}} - \frac{RT}{\alpha}\frac{\phi^{w} c^{+} c^{-}}{\gamma_{-} c^{-}}\right]\gamma_{-}\frac{\partial c^{-}}{\partial x} \end{array}\right\} = 0$$

or:

$$\frac{c^{F}}{\alpha}(E + B_{w})\frac{\partial^{2} u}{\partial x^{2}} + \frac{RT}{\alpha}c^{F}(1-\phi)\frac{\partial c^{k}}{\partial x} + D^{+}\frac{\partial c^{+}}{\partial x} - D^{-}\frac{\partial c^{-}}{\partial x} = 0 \tag{3.2.7}$$

which is the third constitutive equation for the model, where D^{+} and D^{-} are the diffusivities of the cations and anions, respectively.

Applying these simplifications to equation (3.1.9), it becomes

$$\frac{\partial(\phi^{w} c^{k})}{\partial \mathrm{t}} - \frac{\partial}{\partial x}\left\{\begin{array}{c} \frac{RT}{\alpha}\phi^{w} c^{k}\frac{\partial}{\partial x}\left[\frac{p}{RT} - \phi c^{k} + \frac{B_{w}}{RT}\frac{\partial u}{\partial x}\right] \\ +\phi^{w}\left[\frac{c^{+} D^{+}}{\gamma_{+} c^{+}} + \frac{RT}{\alpha}\frac{(c^{+})^{2}}{\gamma_{+} c^{+}} + \frac{RT}{\alpha}\frac{c^{+} c^{-}}{\gamma_{+} c^{+}}\right]\gamma_{+}\frac{\partial c^{+}}{\partial x} \\ +\phi^{w}\left[\frac{c^{-} D^{-}}{\gamma_{-} c^{-}} + \frac{RT}{\alpha}\frac{(c^{-})^{2}}{\gamma_{-} c^{-}} + \frac{RT}{\alpha}\frac{c^{+} c^{-}}{\gamma_{-} c^{-}}\right]\gamma_{-}\frac{\partial c^{-}}{\partial x} \end{array}\right\} + \frac{\partial}{\partial x}\left(\phi^{w} c^{k}\frac{\partial u}{\partial t}\right) = 0$$

which reduces to:

$$\frac{\partial(\phi^w c^k)}{\partial \mathrm{t}} = \frac{\partial}{\partial x}\left\{\begin{array}{c}\frac{E+B_w}{\alpha}[\phi^w - (\phi^w)^2]c^k\frac{\partial^2 u}{\partial x^2} + \frac{RT}{\alpha}(1-\phi)[\phi^w - (\phi^w)^2]c^k\frac{\partial c^k}{\partial x} \\ +\phi^w\left(D^+\frac{\partial c^+}{\partial x} + D^-\frac{\partial c^-}{\partial x}\right)\end{array}\right\} \quad (3.2.8)$$

Equation (3.2.8) is the fourth constitutive equation of the model.

Written all together, the four equations of our model in one-dimensional form are:

$$p = E\frac{\partial u}{\partial x} \quad (3.2.3)$$

$$\frac{\partial u}{\partial t} = \frac{E+B_w}{\alpha}\phi^w\frac{\partial^2 u}{\partial x^2} + \frac{RT}{\alpha}\phi^w(1-\phi)\frac{\partial c^k}{\partial x} \quad (3.2.6)$$

$$\frac{c^F}{\alpha}(E+B_w)\frac{\partial^2 u}{\partial x^2} + \frac{RT}{\alpha}c^F(1-\phi)\frac{\partial c^k}{\partial x} + D^+\frac{\partial c^+}{\partial x} - D^-\frac{\partial c^-}{\partial x} = 0 \quad (3.2.7)$$

$$\frac{\partial(\phi^w c^k)}{\partial \mathrm{t}} = \frac{\partial}{\partial x}\left\{\begin{array}{c}\frac{E+B_w}{\alpha}[\phi^w - (\phi^w)^2]c^k\frac{\partial^2 u}{\partial x^2} + \frac{RT}{\alpha}(1-\phi)[\phi^w - (\phi^w)^2]c^k\frac{\partial c^k}{\partial x} \\ +\phi^w\left(D^+\frac{\partial c^+}{\partial x} + D^-\frac{\partial c^-}{\partial x}\right)\end{array}\right\} \quad (3.2.8)$$

3.2.3 Multiscaling

As mentioned in section 2.6, the multiscaling method used in this model follows the technique laid out by Peter and Böhm[15]. This method is used to predict macroscopic behavior from microscopic structure, linking the two different scales. In order to describe the relationship between the two scales, the characteristic variables associated with each scale must be defined. The characteristic microscopic length is defined as ℓ, and the characteristic macroscopic length is defined as L. They are related by:

$$\varepsilon = \frac{\ell}{\mathrm{L}} \quad (3.2.9)$$

which must satisfy $\varepsilon \ll 1$, because the microscopic scale is significantly smaller than the macroscopic scale. There are also lengths associated with the diffusion of the cation and anion species, which are denoted as ℓ^+ and ℓ^-, respectively. These are defined by the relation:

$$\ell^\alpha = \sqrt{\mathrm{H}_\alpha}\ell \quad (3.2.10)$$

where α is either + or – for cations or anions, respectively. H_+ and H_- are scales that will be defined later.

Not only do the microscopic and macroscopic scales differ with respect to length, but they also differ with respect to time. The characteristic time for the deformation of the solid phase is τ, and the characteristic diffusion times for cations and anions follow the equations

$$\tau^+ = \frac{(\ell^+)^k L^{2-k}}{D_0}, \tau^- = \frac{(\ell^-)^j L^{2-j}}{D_0} \qquad (3.2.11, 3.2.12)$$

where $k, j \in [0,2]$ are scaling parameters, which are defined so that the characteristic diffusion times for all ion species are equal to the diffusion time for the fastest-diffusing species. D_0 is the characteristic diffusivity for the tissue under consideration.

3.2.4 Accounting for Ion Interactions

Unlike the model described in the paper by Sun et al.[17], this model takes into the production and consumption of ions into account. This method can also account for abnormal behavior in the tissue, as well, such as tumors. Therefore, the following system is proposed, modified from the set of constitutive equations (3.2.3), (3.2.6)-(3.2.8):

$$p = E\frac{\partial u}{\partial x} \qquad (3.2.13)$$

$$\frac{\partial u}{\partial t} = \frac{E+B_w}{\alpha}\phi^w \frac{\partial^2 u}{\partial x^2} + \frac{RT}{\alpha}\phi^w(1-\phi)\left(\frac{\partial c^+}{\partial x} + \frac{\partial c^-}{\partial x}\right) \qquad (3.2.14)$$

$$\frac{\partial}{\partial t}(\phi^w c^+) + \frac{\partial}{\partial x}\begin{bmatrix} -\frac{RT}{\alpha}\phi^w c^+ \frac{\partial \varepsilon^w}{\partial x} \\ -\left(\phi^w D^+ + \frac{RT}{\alpha}\phi^w c^+\right)\frac{\partial c^+}{\partial x} \\ -\frac{RT}{\alpha}\phi^w c^+ \frac{\partial c^-}{\partial x} \end{bmatrix} + \frac{\partial}{\partial x}\left(\phi^w c^+ \frac{\partial u}{\partial t}\right) = -R^+ f \qquad (3.2.15)$$

$$\frac{\partial}{\partial t}(\phi^w c^-) + \frac{\partial}{\partial x}\begin{bmatrix} -\frac{RT}{\alpha}\phi^w c^- \frac{\partial \varepsilon^w}{\partial x} \\ -\left(\phi^w D^- + \frac{RT}{\alpha}\phi^w c^-\right)\frac{\partial c^-}{\partial x} \\ -\frac{RT}{\alpha}\phi^w c^- \frac{\partial c^+}{\partial x} \end{bmatrix} + \frac{\partial}{\partial x}\left(\phi^w c^- \frac{\partial u}{\partial t}\right) = R^- f \qquad (3.2.16)$$

where R^+, R^-, f are associated with the consumption/production rates of ions. The consumption reactions are assumed to be of the form:

$$n_{\mathrm{A}}\mathrm{A} + n_{\mathrm{B}}\mathrm{B} \rightarrow n_{\mathrm{C}}\mathrm{C}$$

and the production reactions of the form:

$$n_{\mathrm{A}}\mathrm{A} \rightarrow n_{\mathrm{B}}\mathrm{B} + n_{\mathrm{C}}\mathrm{C}$$

where n_A, n_B, n_C are stoichiometric coefficients associated with the ion species. These coefficients are assumed to be of the form:

$$n^+ = R^+ r_+ r_-,\ n^- = R^- r_+ r_- \tag{3.2.17}$$

where r_+ and r_- are functions of the cation concentration and anion concentration, respectively, and R^+, R^- are bounded and associated with the ions' molecular weights and the reaction-rate constant. The quantity f is the concentration-dependent part of the production rate, such that:

$$f = r_+ r_- = (c^+)^p (c^-)^q \tag{3.2.18}$$

where p, q are real numbers, where either $p, q = 0$ or $p, q \geq 1$.

3.2.5 Non-Dimensionalization

Because constitutive equations are intended to describe properties inherent to the material, the equations for this model have been non-dimensionalized. The variables in the equations have all been related to their reference states in the following manner:

$$\tilde{x} = \frac{x}{L}, \qquad t^{\pm} = \frac{t}{\tau^{\pm}}, \qquad \tilde{t} = \frac{t}{\tau}, \qquad \tilde{u} = \frac{u}{L}, \qquad \tilde{p} = \frac{p}{p_0}$$

$$\widetilde{D}^+ = \frac{H_+^{k/2}}{D_0} D^+, \qquad \widetilde{D}^- = \frac{H_-^{j/2}}{D_0} D^-, \qquad \tilde{R}^{\pm} = \frac{\tau^{\pm}}{c_0} R^{\pm}$$

where L is the characteristic macroscopic length, $\tau^{\pm}$ is the characteristic ion diffusion time, τ is the characteristic time of solid deformation, u is the velocity of the solid in the x direction, p is the hydrostatic fluid pressure, and $R^{\pm}$ is related to the consumption/production rates of ions, as will be discussed later. The subscript zero indicates a reference quantity, such as the reference pressure p_0. The tilde above a variable indicates that it has been non-dimensionalized. The superscript $\pm$ indicates that the variables in the equation are either all associated with the cation species (+) or the anion species (–).

3.2.6 Proposed Model

The last simplification of our model was linearization of the equations. For example, it is assumed that the displacement is infinitesimal ($\frac{\partial u}{\partial x} \ll 1$), therefore the higher-order derivatives of u are assumed to be negligibly small. One result of this is that $\frac{\partial p}{\partial x} = E \frac{\partial^2 u}{\partial x^2} = 0$, so there is no pressure gradient in the x direction. For this first approximation, diffusion and convection are also assumed to be linear, therefore products of the concentrations can be neglected as well. The material constant B_w was also assumed to be zero for further simplification. As was discussed in the paper by Peter and

Böhm,[15] it is assumed that the characteristic displacement time of the solid is equal to the ion diffusion times ($\tau = \tau^+ = \tau^-$) and thus $\tilde{t} = t^+ = t^-$.

The final system of constitutive equations for this tri-phasic tissue model is as follows:

$$\frac{\partial \tilde{u}}{\partial \tilde{t}} = \frac{\tau E}{\alpha L^2}(1-\phi_0^s)\frac{\partial^2 \tilde{u}}{\partial \tilde{x}^2} + \frac{\tau RTc_0}{\alpha L^2}(1-\phi)(1-\phi_0^s)\left(\frac{\partial \tilde{c}^+}{\partial \tilde{x}} + \frac{\partial \tilde{c}^-}{\partial \tilde{x}}\right) \tag{3.2.19}$$

$$\frac{\partial \tilde{c}^+}{\partial \tilde{t}} - \varepsilon^k \tilde{D}^+ \frac{\partial^2 \tilde{c}^+}{\partial \tilde{x}^2} + \frac{\partial}{\partial \tilde{x}}\left(\tilde{c}^+ \frac{\partial \tilde{u}}{\partial \tilde{t}}\right) = -K\tilde{R}^+\tilde{f} \tag{3.2.21}$$

$$\frac{\partial \tilde{c}^-}{\partial \tilde{t}} - \varepsilon^j \tilde{D}^- \frac{\partial^2 \tilde{c}^-}{\partial \tilde{x}^2} + \frac{\partial}{\partial \tilde{x}}\left(\tilde{c}^- \frac{\partial \tilde{u}}{\partial \tilde{t}}\right) = +K\tilde{R}^-\tilde{f} \tag{3.2.20}$$

where $K = (1-\phi_0^s)^{-1}$and $\tau = \frac{H_+^{k/2}\ell^k L^{2-k}}{D_0} = \frac{H_-^{j/2}\ell^j L^{2-j}}{D_0}$. Zero Neumann conditions are assumed on the solid-liquid phase interfaces and the ionic-liquid phase interface ($\Gamma^{\mathrm{sw}}, \Gamma^{\mathrm{iw}}$). At $t = 0$, the tissue is assumed to be periodic with respect to a reference cell denoted by $Y = (0,1)$ containing the three phases. The reference or unit cell is scaled by $\varepsilon = \frac{\ell}{L} \ll 1$. The change from a periodic domain to an evolving domain, which is part of the multiscaling process as described in Section 2.6, is seen as a union of a finite number of εY cells. This is described by orientation-preserving mappings $\psi_\varepsilon^a(\cdot, t): \Omega^a \to \Omega^{a\prime}$, where $a \in \{s, w, i\}$, and Ω^a denotes the domain of one of the three phases. This is denoted by $\psi_\varepsilon^a = \nabla\psi_\varepsilon^a, J_\varepsilon^a = \det\psi_\varepsilon^a$. In the next section, these constitutive equations are used in a very simple case study to examine the effects of ion diffusion on the solid phase.

Chapter 4. Implementation

After designing the model, two very simple situations were considered as a preliminary test: the effects of (1) pure macroscopic ion diffusion and (2) pure microscopic ion diffusion on solid displacement.

4.1 Initial and Boundary Conditions

Let the periodic domain be the interval (0,1). Let the characteristic lengths be the following values: macroscopic length L = 1, microscopic length $\ell = 10^{-4}$, and $H_+ = H_- = 0.1$ so that $\ell^+ = \ell^- = 3.2 * 10^{-5}$. Therefore, the condition that $\varepsilon = \frac{\ell}{L} \ll 1$ is satisfied. Let the characteristic time for solid deformation be $\tau = 1$. The effective physical parameters in the model are not the focus of this test, therefore they are taken to be unity. These include $E, D^+, D^-, R, T, \alpha, \phi$, and ϕ_0^s, which listed in order are as follows: the Young's modulus of the solid, the diffusivities of the cations and anions, the universal gas constant, the absolute temperature, a constant related to hydraulic permeability, the osmotic coefficient, and the initial volume fraction of the solid phase. Setting these to unity means that the non-dimensionalized cation and anion concentrations are equivalent: $\tilde{c}^+ = \tilde{c}^- = \tilde{c}$.

The scaling parameters k, j used in calculating the non-dimensionalized ion diffusivities are different for the two cases:

1. Pure macroscopic diffusion: $\widetilde{D}^+ = \widetilde{D}^- = 1 \rightarrow k = j = 0$
2. Pure microscopic diffusion: $\widetilde{D}^+ = \widetilde{D}^- = 10^{-9} \rightarrow k = j = 2$

In both cases, the following initial and boundary conditions for non-dimensionalized displacement and concentration are assumed:

$$\tilde{u}(\tilde{x}, 0) = \tilde{u}(0, \tilde{t}) = \tilde{u}(1, \tilde{t}) = 0 \tag{4.1.1}$$

$$\tilde{c}(\tilde{x}, 0) = \mathrm{e}^{-10(\tilde{x}-0.5)^2} \tag{4.1.2}$$

$$\tilde{c}(0, \tilde{t}) = \tilde{c}(1, \tilde{t}) = \mathrm{e}^{-5/2} \tag{4.1.3}$$

4.2 Results

In case 1, the macroscopic diffusion had a noticeable though relatively small effect on the solid phase. Figure 4.1.1 demonstrates the initial concentration field considered in this case over the solid length and its change over time. The concentration field is increased as specified in the initial conditions and decreases to equilibrium over time. Figure 4.1.2 shows the effect on the solid phase's displacement. As can be seen, there is shrinkage of the solid phase in regions corresponding to the initial increases in

ion concentration, on the order of 10^{-3} of the macroscopic length. As the concentration returns to equilibrium, the solid phase returns to its original size.

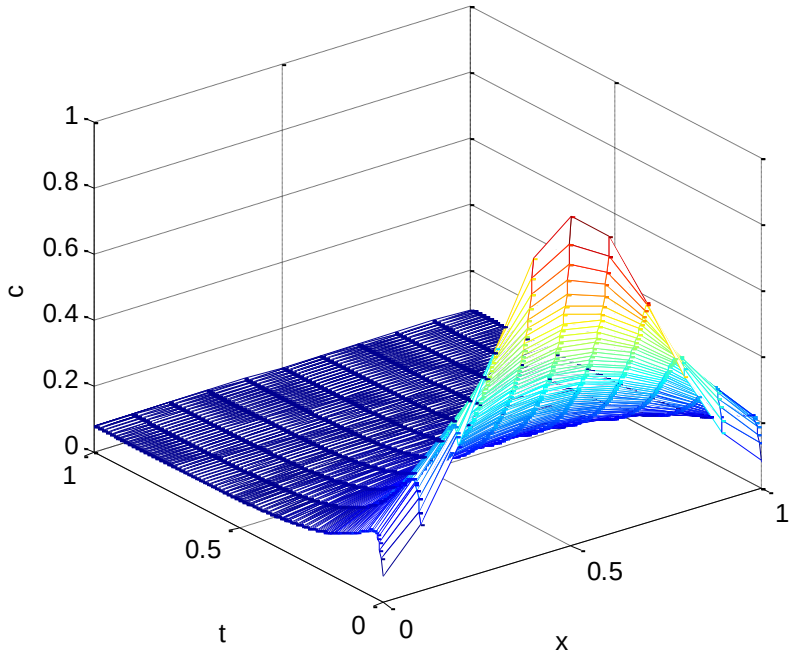

Figure 4.1.1: Concentration field in case 1

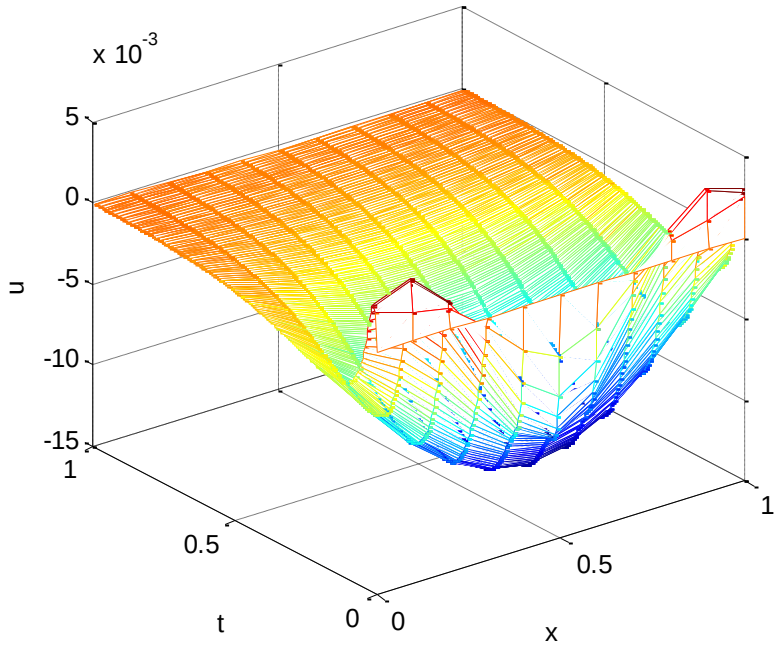

Figure 4.1.2: Displacement field of the solid phase in case 1

In case 2, no macroscopic diffusion resulted from the initial microscopic diffusion condition, because the concentration field depends only on the macroscopic variable $\tilde{x}$ and not the microscopic variable $\tilde{x}/\varepsilon$. No displacement of the solid phase resulted from only microscopic diffusion. Because there was neither a macroscopic change in the concentration nor a macroscopic change in the solid displacement, figures were not included for case 2.

4.3 Discussion

The results from these very basic cases may be able to be used as a simplistic set-up for tumor modeling and classification. As discussed in Section 2.5, there are significant differences in biology between benign and malignant tumors. One hypothesis is that although benign tumor cells are encapsulated, they are not significantly different in ion transport from healthy cells[2]. Malignant tumor cells, however, differ both in morphology and ion transport from healthy and benign cells. One possible theory is that benign tumors only undergo microscopic diffusion and therefore do not have macroscopic deformation of the solid phase (as in the second case considered in Section 4.2). Malignant tumors, on the other hand, undergo macroscopic diffusion and cell shrinkage, which possibly would make them stiffer. This would agree with the results of the study by Drapaca and Palocaren,[3] which indicated that cancerous tumors are stiffer than benign tumors. Assuming that macroscopic diffusion is characteristic of malignant and not benign tumors also agrees with the physiological fact that malignant tumors initiate angiogenesis and benign tumors do not. The new blood vessels supply the cancerous tumor with a large supply of nutrients and ions. A more complete analysis of the diffusion involved could provide vital information about the transformation of a tumor from benign to malignant. This information could be used in a more complex computational model which will be created in future work to enable the non-invasive characterization of tumors through Magnetic Resonance Elastography.

Chapter 5. Conclusion

5.1 Summary

In this thesis, a novel multiscale triphasic model for biological tissues was proposed that is based on the method of homogenization of domains with evolving microstructure. The specific focus for this and future models is on brain tissue. Therefore, the three phases correlated to cell membranes and structural proteins for the solid phase, cerebrospinal fluid for the liquid phase, and blood for the ion phase. The intent of this research was to create a model which could describe healthy and diseased brain tissue, and possibly differentiate between benign and malignant tumors. The very preliminary results from the implementation of two simple diffusion cases show promise in obtaining better and more complicated models in order to reliably identify and classify tumors using Magnetic Imaging Elastography.

5.2 Future Work

Future work consists of both more accurate model design and applications of the models. Future models will be designed in two and three dimensions, since this model was only in one dimension. As more research is conducted on these models, they will also be able to more closely approximate the actual brain tissue. For example, ion transport between the cerebrospinal fluid and the circulatory system could be accounted for, instead of assumed to be zero. In order to test the accuracy of these models, both computer simulations and *in vitro* testing of healthy brain tissue and glioma samples will be performed. Eventually, the model will be able to be translated into code for use with Magnetic Resonance Elastography, and clinical testing of the model will then be able to be conducted.

Bibliography

1. Dong C. Class Lecture. Bio-Continuum Mechanics. The Pennsylvania State University. University Park, PA.
2. Drapaca CS. Private Discussions and Personal Notes. Senior Research and Design Project II, Honors. The Pennsylvania State University. University Park, PA.
3. Drapaca CS, Palocaren AJ. (2010) *Biomechanical modeling of tumor classification and growth*, Rev. Roum. Sci. Tech. – Mec. Appl., 55(2):115-124.
4. Duck FA. Physical Properties of Tissues – A Comprehensive Reference Book. 6th Ed. Sheffield, UK: Academic, 1990.
5. Friedman MH. *Principles and Models of Biological Transport*. 2nd Ed. Springer-Science +Business Media LLC, New York: 2008
6. Fung YC. Biomechanics – Mechanical Properties of Living Tissues. 2nd Ed. Springer, New York, 1993.
7. Gu WY, Lai WM and Mow VC. (1998) *A mixture theory for charged-hydrated soft tissues containing multi-electrolytes: passive transport and swelling behaviors*. J. Biomech. Engrg. 120: 169-180.
8. Hilbert D. *The Foundations of Geometry*. Translation by Townsend, E.J. The Open Court Publishing Co., La Salle, Illinois, 1950.
9. Kruse S.A. et al. (2008) *Magnetic resonance elastography of the brain*. Neuroimage 39:231–237.
10. Lodish et al. *Molecular Cell Biology*. 6th Ed. W.H. Freeman & Co., New York: 2008.
11. Muthupillai R, Lomas DJ, Rossman PJ, Greenleaf JF, Manduca A, and Ehman RL. (1995) *Magnetic resonance elastography by direct visualization of propagating acoustic strain waves*. Science 269: 1854-1857.
12. Muthupillai R, Rossman PJ, Lomas DJ, Greenleaf JF, Riederer SJ, and Ehman RL. (1996) *Magnetic resonance imaging of transverse acoustic strain waves*, Magn. Reson. Med. 36: 266-274.
13. Peter MA. (2007) *Homogenization in domains with evolving microstructure*. C.R. Mecanique 335: 357-362.
14. Peter MA. (2007) *Homogenization of a chemical degradation mechanism inducing an evolving microstructure*. C.R. Mecanique, 335: 679-684.
15. Peter MA, Böhm M. (2009) *Multiscale modeling of chemical degradation mechanisms in porous media with evolving microstructure*. Multiscale Model. Simul. 7(4): 1643-1668.
16. Ratner, B.D., Ed. *Biomaterials Science: An Introduction to Materials in Medicine*. 2nd Ed. Elsevier Academic Press, New York: 2004.
17. Sun DN, Gu WY, Guo XE, Lai WM, and Mow VC. (1999) *A mixed finite element formulation of triphasic mechano-electrochemical theory for charged, hydrated biological soft tissues*. Int. J. Numer. Meth. Engng. 45: 1375-1402.
18. Tortora GJ, Derrickson B. *Principles of Anatomy and Physiology*. 11th Ed. J.W. Wiley & Sons: 2006.
19. Taber L.A. *Nonlinear Theory of Elasticity: Applications in Biomechanics*. World Scientific Publishing Co. Pte. Ltd.: 2004.

Academic Vita of Kathryn I. Barber

Education

The Pennsylvania State University, University Park, PA

- Graduation date: May 2011
- Bachelor of Science in Engineering Science with Honors and a minor in Bioengineering
- Undergraduate Thesis: *Design of a tri-phasic multi-scaling model for healthy and cancerous tissue mechanics,* under thesis supervisor Corina Drapaca
- Member of the Schreyer Honors College and The Honor Society of Phi Kappa Phi

Publications

Kathryn Barber and Corina Drapaca, Ph.D. *A multiscale triphasic biomechanical model for tumors' classification.* Abstract accepted to the 1st International Symposium on the Mechanics of Biological Systems and Materials, part of the 2011 SEM Conference and Exposition on Experimental and Applied Mechanics at the Mohegan Sun, Uncasville, CT USA June 13-15, 2011.

Kathryn Barber and Corina Drapaca, Ph.D. *A multiscale triphasic biomechanical model for brain tumors' classification.* Abstract accepted to the 7th International Congress on Industrial and Applied Mathematics (ICIAM 2011) at the Vancouver Convention Centre, Vancouver, BC, Canada July 18-22, 2011.

Select Awards

The Evan Pugh Scholar Award 2011

The President's Freshman Award 2008

Prestigious Scholarships

Barry M. Goldwater Scholarship 2009-2011

National Merit Scholarship, sponsored by 3M Company 2007-2008

Research Experience

University of Delaware, Newark, DE June 8 – August 14, 2009

Nature-InSpired Engineering Research Experience for Undergraduates (NSF-sponsored)

- Synthesized polymer-peptide hydrogels to serve as tunable scaffolds for vocal fold tissue regeneration
- Presented a poster at the Summer Undergraduate Research Symposium at the University of Delaware on August 12, 2009

The Pennsylvania State University, University Park, PA Feb 2008 – June 2009

Mechanical Engineering Undergraduate Research Assistant

- Designed, analyzed, and constructed a prototype of the controls of a suturing device for Natural Orifice Transluminal Endoscopic Surgery
- One of four Penn State students selected to present a poster at Undergraduate Research at the Capitol in Harrisburg on October 7, 2008